J|A|C|S
ARTICLES

Published on Web 08/27/2009

# Chemically Converted Graphene Induced Molecular Flattening of 5,10,15,20-Tetrakis(1-methyl-4-pyridinio)porphyrin and Its Application for Optical Detection of Cadmium(II) Ions

Yuxi Xu, Lu Zhao, Hua Bai, Wenjing Hong, Chun Li, and Gaoquan Shi*

*Key Laboratory of Bioorganic Phosphorus Chemistry & Chemical Biology, Department of Chemistry, Tsinghua University, Beijing 100084, People's Republic of China*

Received June 19, 2009; E-mail: gshi@tsinghua.edu.cn

***Abstract:*** Complexation of cationic 5,10,15,20-tetrakis(1-methyl-4-pyridinio)porphyrin (TMPyP) and negatively charged chemically converted graphene (CCG) sheets was performed by simply mixing the diluted aqueous solutions of both components. During this process, a large bathochromic shift of porphyrin Soret band from 421 to 458 nm was observed, which is attributed to the flattening of TMPyP molecules induced by CCG through electrostatic and $\pi-\pi$ stacking cooperative interactions. Furthermore, the coordination reaction between TMPyP and $Cd^{2+}$ ions was greatly accelerated from 20 h to 8 min under ambient conditions by introducing CCG sheets. On the basis of this phenomenon, we used the complex of TMPyP and CCG as an optical probe for rapid and selective detection of $Cd^{2+}$ ions in aqueous media.

## Introduction

Graphene, a two-dimensional (2D) single layer of graphite, has attracted an intense interest in recent years, owing to its unique structure and properties, including high electronic[1] and thermal[2] conductivities, great mechanical strength,[3] and huge specific surface area.[4] Up-to-date, various effective techniques have been developed for producing graphene. Micromechanical exfoliation,[5] epitaxial growth,[6] and chemical vapor deposition[7] can produce graphene with high quality for fundamental studies and potential applications in nanoelectronics. Different from these three approaches, synthesis of graphene colloidal dispersions using graphite,[8,9] graphite oxide (GO),[10−19] or other graphite derivatives[20−22] as starting materials not only can be scalable but also can provide graphene with processability and new functions. Since GO can be readily dispersed as individual sheets in its good solvents,[23,24] most colloidal dispersions of graphene were prepared by reduction of GO suspensions.[25] Although chemical reduction can eliminate a majority of the oxygen functional groups and restore the conjugated structure of GO, the structure of chemically converted graphene (CCG) is still disordered to some extent compared with that of ideal graphene. Colloidal dispersions of CCG have shown many promising applications such as energy-storage materials,[4,26]

(1) Geim, A. K.; Novoselov, K. S. *Nat. Mater.* **2007**, *6*, 183–191.
(2) Balandin, A. A.; Ghosh, S.; Bao, W. Z.; Calizo, I.; Teweldebrhan, D.; Miao, F.; Lau, C. N. *Nano Lett.* **2008**, *8*, 902–907.
(3) Lee, C.; Wei, X. D.; Kysar, J. W.; Hone, J. *Science* **2008**, *321*, 385–388.
(4) Stoller, M. D.; Park, S. J.; Zhu, Y. W.; An, J. H.; Ruoff, R. S. *Nano Lett.* **2008**, *8*, 3498–3502.
(5) Novoselov, K. S.; Geim, A. K.; Morozov, S. V.; Jiang, D.; Zhang, Y.; Dubonos, S. V.; Grigorieva, I. V.; Firsov, A. A. *Science* **2004**, *306*, 666–669.
(6) Berger, C.; Song, Z. M.; Li, X. B.; Wu, X. S.; Brown, N.; Naud, C.; Mayou, D.; Li, T. B.; Hass, J.; Marchenkov, A. N.; Conrad, E. H.; First, P. N.; de Heer, W. A. *Science* **2006**, *312*, 1191–1196.
(7) Kim, K. S.; Zhao, Y.; Jang, H.; Lee, S. Y.; Kim, J. M.; Ahn, J. H.; Kim, P.; Choi, J. Y.; Hong, B. H. *Nature* **2009**, *457*, 706–710.
(8) Hernandez, Y.; et al. *Nat. Nanotechnol.* **2008**, *3*, 563–568.
(9) Lotya, M.; Hernandez, Y.; King, P. J.; Smith, R. J.; Nicolosi, V.; Karlsson, L. S.; Blighe, F. M.; De, S.; Wang, Z. M.; McGovern, I. T.; Duesberg, G. S.; Coleman, J. N. *J. Am. Chem. Soc.* **2009**, *131*, 3611–3620.
(10) Schniepp, H. C.; Li, J. L.; McAllister, M. J.; Sai, H.; Herrera-Alonso, M.; Adamson, D. H.; Prud'homme, R. K.; Car, R.; Saville, D. A.; Aksay, I. A. *J. Phys. Chem. B* **2006**, *110*, 8535–8539.
(11) McAllister, M. J.; Li, J. L.; Adamson, D. H.; Schniepp, H. C.; Abdala, A. A.; Liu, J.; Herrera-Alonso, M.; Milius, D. L.; Car, R.; Prud'homme, R. K.; Aksay, I. A. *Chem. Mater.* **2007**, *19*, 4396–4404.
(12) Li, D.; Muller, M. B.; Gilje, S.; Kaner, R. B.; Wallace, G. G. *Nat. Nanotechnol.* **2008**, *3*, 101–105.
(13) Park, S.; An, J. H.; Piner, R. D.; Jung, I.; Yang, D. X.; Velamakanni, A.; Nguyen, S. T.; Ruoff, R. S. *Chem. Mater.* **2008**, *20*, 6592–6594.
(14) Chen, H.; Muller, M. B.; Gilmore, K. J.; Wallace, G. G.; Li, D. *Adv. Mater.* **2008**, *20*, 3557–3561.
(15) Park, S.; An, J. H.; Jung, I. W.; Piner, R. D.; An, S. J.; Li, X. S.; Velamakanni, A.; Ruoff, R. S. *Nano Lett.* **2009**, *9*, 1593–1597.
(16) Tung, V. C.; Allen, M. J.; Yang, Y.; Kaner, R. B. *Nat. Nanotechnol.* **2009**, *4*, 25–29.
(17) Wang, G. X.; Yang, J.; Park, J.; Gou, X. L.; Wang, B.; Liu, H.; Yao, J. *J. Phys. Chem. C* **2008**, *112*, 8192–8195.
(18) Fan, X. B.; Peng, W. C.; Li, Y.; Li, X. Y.; Wang, S. L.; Zhang, G. L.; Zhang, F. B. *Adv. Mater.* **2008**, *20*, 4490–4493.
(19) Wu, Z. S.; Ren, W. C.; Gao, L. B.; Zhao, J. P.; Chen, Z. P.; Liu, B. L.; Tang, D. M.; Yu, B.; Jiang, C. B.; Cheng, H. M. *ACS Nano* **2009**, *3*, 411–417.
(20) Worsley, K. A.; Ramesh, P.; Mandal, S. K.; Niyogi, S.; Itkis, M. E.; Haddon, R. C. *Chem. Phys. Lett.* **2007**, *445*, 51–56.
(21) Valles, C.; Drummond, C.; Saadaoui, H.; Furtado, C. A.; He, M.; Roubeau, O.; Ortolani, L.; Monthioux, M.; Penicaud, A. *J. Am. Chem. Soc.* **2008**, *130*, 15802–15804.
(22) Li, X. L.; Wang, X. R.; Zhang, L.; Lee, S. W.; Dai, H. J. *Science* **2008**, *319*, 1229–1232.
(23) Stankovich, S.; Dikin, D. A.; Piner, R. D.; Kohlhaas, K. A.; Kleinhammes, A.; Jia, Y.; Wu, Y.; Nguyen, S. T.; Ruoff, R. S. *Carbon* **2007**, *45*, 1558–1565.
(24) Paredes, J. I.; Villar-Rodil, S.; Martinez-Alonso, A.; Tascon, J. M. D. *Langmuir* **2008**, *24*, 10560–10564.
(25) Park, S.; Ruoff, R. S. *Nat. Nanotechnol.* **2009**, *4*, 217–224.
(26) Yoo, E.; Kim, J.; Hosono, E.; Zhou, H.; Kudo, T.; Honma, I. *Nano Lett.* **2008**, *8*, 2277–2282.


**10.1021/ja905032g CCC: $40.75** 

polymer composites,[27,28] transparent conducting electrodes,[29−31] electrocatalysis,[32−35] field effect devices,[36−38] and paperlike materials.[12−15,39]

On the other hand, covalent or noncovalent functionalization of graphene with various molecules and nanomaterials has been considered to be important to graphene processing,[39−50] drug delivery,[51] biological sensors,[52,53] and tuning electronic properties of graphene.[54] As a kind of well-known functional dye, porphyrin derivatives also have been used for modifying carbon nanotubes to achieve novel optoelectronic properties.[55] Recently, a graphene hybrid material covalently functionalized with porphyrin also has been synthesized and exhibited excellent optical limiting property.[56] Since CCG sheets in aqueous dispersion are negatively charged,[12] it is expected that CCG sheets can act like a 2D conjugated polyelectrolyte and cationic porphyrin derivatives can be assembled onto their surfaces through electrostatic and $\pi-\pi$ stacking interactions.

In this article, we report the supramolecular assembly or complexation of CCG sheets and cationic 5,10,15,20-tetrakis(1-methyl-4-pyridinio)porphyrin (TMPyP) in aqueous media. An unexpected large flattening of TMPyP molecules adsorbed on CCG sheets was observed. Furthermore, the flattening of TMPyP in the complex of TMPyP and CCG (TMPyP/CCG) greatly accelerated the incorporation of $Cd^{2+}$ ions into TMPyP rings. Thus, the optical sensor based on TMPyP/CCG complex showed rapid and selective responses toward $Cd^{2+}$ ions in aqueous media.

## Experimental Section

**Materials.** Natural graphite powder (325 mesh) was purchased from Tianjing Guangfu Research Institute. 5,10,15,20-Tetrakis(1-methyl-4-pyridinio)porphyrin (TMPyP) tetra(*p*-toluenesulfonate) was bought from TCI. Hydrazine monohydrate (98%), 5,10,15,20-tetrakis(4-trimethylammoniophenyl)porphyrin (TMAP) tetra(*p*-toluenesulfonate), and 5,10,15,20-tetrakis(4-sulfophenyl)porphyrin (TPPS) tetrasodium hydrate were purchased from Sigma-Aldrich. All metal salts were of analytical grade and obtained from Beijing Chemical Reagent Co. Except mercury acetate, the other metal salts were chlorides. Deionized water was used throughout the experiments. All reagents described above were used as received without further purification.

**Graphite Oxide Synthesis and Purification.** GO was prepared by oxidation of natural graphite powder (325 mesh, Tianjing) according to the method developed by Hummers and Offemann.[57] The details are described as follows. Graphite (3.0 g) was added to concentrated sulfuric acid (70 mL) under stirring at room temperature, then sodium nitrate (1.5 g) was added, and the mixture was cooled to 0 °C. Under vigorous agitation, potassium permanganate (9.0 g) was added slowly to keep the temperature of the suspension lower than 20 °C. Successively, the reaction system was transferred to a 35 ± 5 °C water bath and stirred for about 0.5 h, forming a thick paste. Then, 150 mL of water was added, and the solution was stirred for 15 min at 90 ± 5 °C. Additional 500 mL of water was added and followed by a slow addition of 15 mL of $H_2O_2$ (3%), turning the color of the solution from dark brown to yellow. The mixture was filtered and washed with 1:10 HCl aqueous solution (250 mL) to remove metal ions followed by washing with 200 mL of water to remove the acid. The resulting solid was dried in air and diluted to make a GO aqueous dispersion (0.5% w/w). Finally, it was purified by dialysis for one week to remove the remaining metal species.

**Preparation of Aqueous Dispersion of Chemically Converted Graphene and 1-Methyl-2-pyrrolidinone (NMP) Dispersion of Neutral Graphene (NG).** CCG was prepared through the procedures reported by Li and co-workers.[12] The details are described as follows. Fifty milliliters (0.25 mg/mL) of purified GO dispersion was mixed with 14 $\mu$L of hydrazine monohydrate and 150 $\mu$L of ammonia solution (28 wt % in water). The mixture was stirred at 95 °C for 1 h. After reduction, a homogeneous black dispersion with a small amount of black precipitate was obtained. Successively, this dispersion was filtered through glass cotton to remove the precipitate and yield a stable black aqueous dispersion of CCG. The obtained product was characterized by UV−visible spectra and X-ray photoelectron spectra (XPS) (Figures S1 and S2 in the Supporting Information).

The NMP dispersion of NG sheets was also prepared according to the literature.[8] Natural graphite powder was dispersed in NMP at a concentration of 0.1 mg/mL by sonicating for 30 min. The resultant dispersion was then centrifuged at 500 rpm for 90 min.

(27) Stankovich, S.; Dikin, D. A.; Dommett, G. H. B.; Kohlhaas, K. M.; Zimney, E. J.; Stach, E. A.; Piner, R. D.; Nguyen, S. T.; Ruoff, R. S. *Nature* **2006**, *442*, 282–286.
(28) Ramanathan, T.; Abdala, A. A.; Stankovich, S.; Dikin, D. A.; Herrera-Alonso, M.; Piner, R. D.; Adamson, D. H.; Schniepp, H. C.; Chen, X.; Ruoff, R. S.; Nguyen, S. T.; Aksay, I. A.; Prud'homme, R. K.; Brinson, L. C. *Nat. Nanotechnol.* **2008**, *3*, 327–331.
(29) Wang, X.; Zhi, L. J.; Mullen, K. *Nano Lett.* **2008**, *8*, 323–327.
(30) Becerril, H. A.; Mao, J.; Liu, Z.; Stoltenberg, R. M.; Bao, Z.; Chen, Y. *ACS Nano* **2008**, *2*, 463–470.
(31) Tung, V. C.; Chen, L. M.; Allen, M. J.; Wassei, J. K.; Nelson, K.; Kaner, R. B.; Yang, Y. *Nano Lett.* **2009**, *9*, 1949–1955.
(32) Hong, W. J.; Xu, Y. X.; Lu, G. W.; Li, C.; Shi, G. Q. *Electrochem. Commun.* **2008**, *10*, 1555–1558.
(33) Si, Y. C.; Samulski, E. T. *Chem. Mater.* **2008**, *20*, 6792–6797.
(34) Xu, C.; Wang, X.; Zhu, J. W. *J. Phys. Chem. C* **2008**, *112*, 19841–19845.
(35) Seger, B.; Kamat, P. V. *J. Phys. Chem. C* **2009**, *113*, 7990–7995.
(36) Gilje, S.; Han, S.; Wang, M.; Wang, K. L.; Kaner, R. B. *Nano Lett.* **2007**, *7*, 3394–3398.
(37) Luo, Z. T.; Lu, Y.; Somers, L. A.; Johnson, A. T. C. *J. Am. Chem. Soc.* **2009**, *131*, 898–899.
(38) Eda, G.; Fanchini, G.; Chhowalla, M. *Nat. Nanotechnol.* **2008**, *3*, 270–274.
(39) Xu, Y. X.; Bai, H.; Lu, G. W.; Li, C.; Shi, G. Q. *J. Am. Chem. Soc.* **2008**, *130*, 5856–5857.
(40) Stankovich, S.; Piner, R. D.; Chen, X. Q.; Wu, N. Q.; Nguyen, S. T.; Ruoff, R. S. *J. Mater. Chem.* **2006**, *16*, 155–158.
(41) Niyogi, S.; Bekyarova, E.; Itkis, M. E.; McWilliams, J. L.; Hamon, M. A.; Haddon, R. C. *J. Am. Chem. Soc.* **2006**, *128*, 7720–7721.
(42) Li, X. L.; Zhang, G. Y.; Bai, X. D.; Sun, X. M.; Wang, X. R.; Wang, E.; Dai, H. J. *Nat. Nanotechnol.* **2008**, *3*, 538–542.
(43) Bai, H.; Xu, Y. X.; Zhao, L.; Li, C.; Shi, G. Q. *Chem. Commun.* **2009**, 1667–1669.
(44) Williarris, G.; Seger, B.; Kamat, P. V. *ACS Nano* **2008**, *2*, 1487–1491.
(45) Hao, R.; Qian, W.; Zhang, L. H.; Hou, Y. L. *Chem. Commun.* **2008**, 6576–6578.
(46) Liu, N.; Luo, F.; Wu, H. X.; Liu, Y. H.; Zhang, C.; Chen, J. *Adv. Funct. Mater.* **2008**, *18*, 1518–1525.
(47) Shen, J. F.; Hu, Y. H.; Li, C.; Qin, C.; Ye, M. X. *Small* **2009**, *5*, 82–85.
(48) Si, Y.; Samulski, E. T. *Nano Lett.* **2008**, *8*, 1679–1682.
(49) Lomeda, J. R.; Doyle, C. D.; Kosynkin, D. V.; Hwang, W. F.; Tour, J. M. *J. Am. Chem. Soc.* **2008**, *130*, 16201–16206.
(50) Liang, Y. Y.; Wu, D. Q.; Feng, X. L.; Mullen, K. *Adv. Mater.* **2009**, *21*, 1679–1683.
(51) Liu, Z.; Robinson, J. T.; Sun, X. M.; Dai, H. J. *J. Am. Chem. Soc.* **2008**, *130*, 10876–10877.
(52) Mohanty, N.; Berry, V. *Nano Lett.* **2008**, *8*, 4469–4476.
(53) Shan, C. S.; Yang, H. F.; Song, J. F.; Han, D. X.; Ivaska, A.; Niu, L. *Anal. Chem.* **2009**, *81*, 2378–2382.
(54) Chen, W.; Chen, S.; Qi, D. C.; Gao, X. Y.; Wee, A. T. S. *J. Am. Chem. Soc.* **2007**, *129*, 10418–10422.
(55) Guldi, D. M.; Rahman, A.; Sgobba, V.; Ehli, C. *Chem. Soc. Rev.* **2006**, *35*, 471–487.
(56) Xu, Y. F.; Liu, Z. B.; Zhang, X. L.; Wang, Y.; Tian, J. G.; Huang, Y.; Ma, Y. F.; Zhang, X. Y.; Chen, Y. S. *Adv. Mater.* **2009**, *21*, 1275–1279.
(57) Hummers, W. S., Jr.; Offeman, R. E. *J. Am. Chem. Soc.* **1958**, *80*, 1339.

After centrifugation, the top half of the dispersion containing 0.01 mg/mL NG was collected for our studies.

**Characterizations.** UV−visible spectra were recorded on a U-3010 UV−visible spectrometer (Hitachi). Fluorescence spectra were recorded on a Perkin-Elmer LS55 luminescence spectrometer. Atomic force microscopic (AFM) images were taken using a Nanoscope III MultiMode SPM (Digital Instruments) with an AS-12 ("E") scanner operated in tapping mode in conjunction with a V-shaped tapping tip (Applied Nanostructures SPM model: ACTA). The images were recorded at a scan rate of 2 Hz. XPS analyses were performed on a PHI 550 EACA/SAM photoelectron spectrometer (JEOL) using Al Kα (1486.6 eV) radiation.

## Results and Discussion

**Supramolecular Assembly of CCG and TMPyP.** CCG sheets in aqueous dispersion are negatively charged because of their residual carboxyl groups[12] and thus can be viewed as a 2D anionic conjugated polymer. Thus, as a positively charged porphyrin, TMPyP molecules can be assembled onto the surfaces of CCG sheets to form complexes through electrostatic and $\pi-\pi$ stacking interactions. The interplay between CCG sheets and TMPyP molecules during the process of assembly was studied by the use of UV−visible spectroscopy. A 1 $\mu$M aqueous solution of TMPyP was titrated with 0.25 mg/mL (based on the initial GO weight content) of CCG dispersion at room temperature. As shown in Figure 1A, the spectrum of the aqueous solution of TMPyP features an intense Soret band at 421 nm together with four weak Q bands.[58] During the titration process, the intensity of the original Soret band at 421 nm decreased gradually and a new Soret band at 458 nm appeared and intensified with an isosbestic point at 429 nm. In addition, by subtracting the normalized spectrum of pure CCG dispersion from that of the TMPyP/CCG complex, a spectrum that corresponds to the contribution of TMPyP component in TMPyP/CCG complex was obtained (Figure 1B, defined as subtraction spectrum here). It is clear from Figure 1B that the Soret band of the TMPyP/CCG complex formed at the end point of titration exhibits a large bathochromic shift (37 nm), a broader half-bandwidth, and weaker extinction compared with that of pure TMPyP solution. Meanwhile, the absorbance at 458 nm read from the subtraction spectra increases linearly with the mixing amount of CCG dispersion and reaches a maximum after addition of 60 $\mu$L or more of CCG dispersion (Figure 1C). On the basis of the spectral results described above, it is reasonable to conclude that a TMPyP/CCG complex was formed by simply mixing the solutions of both components and TMPyP molecules were extensively adsorbed on CCG sheets at the end point of titration.

**Flattening of TMPyP Molecules Induced by CCG Sheets.** As described above, the Soret band of TMPyP showed a large bathochromic shift (37 nm) after complexation with CCG sheets. This phenomenon can be explained by several mechanisms according to the literature:[59−62] (i) Diprotonation of the porphyrin ring nitrogens,[59] (ii) solvent effect,[60,61] (iii) J-aggregation of porphyrin molecules,[62] and (iv) flattening of porphyrin molecules caused by twist of their cationic methylpyridinium groups.[60] For mechanism (i), the diprotonation of the porphyrin rings can be performed only in a highly acidic medium. The p$K_a$ (at 25 °C) of TMPyP in aqueous solution was reported to be ~1.5,[60] and the pH value of the solution used here was measured to be 7−8; thus, diprotonation mechanism can be ruled out. For mechanism (ii), only small spectral shifts of the Soret band (2−3 nm) were observed for TMPyP in different solvents.[60] Therefore, this mechanism cannot account for the large red-shift (37 nm) observed in our case. For mechanism (iii), J-aggregates of porphyrin molecules exhibit a red-shift of Soret band (8 nm) compared with that of corresponding monomers.[62] However, in this case, several facts do not support this mechanism. First, during the process of titration, a clear isosbestic point at 429 nm was observed and variation of the amount of CCG dispersion used for titration did not affect the

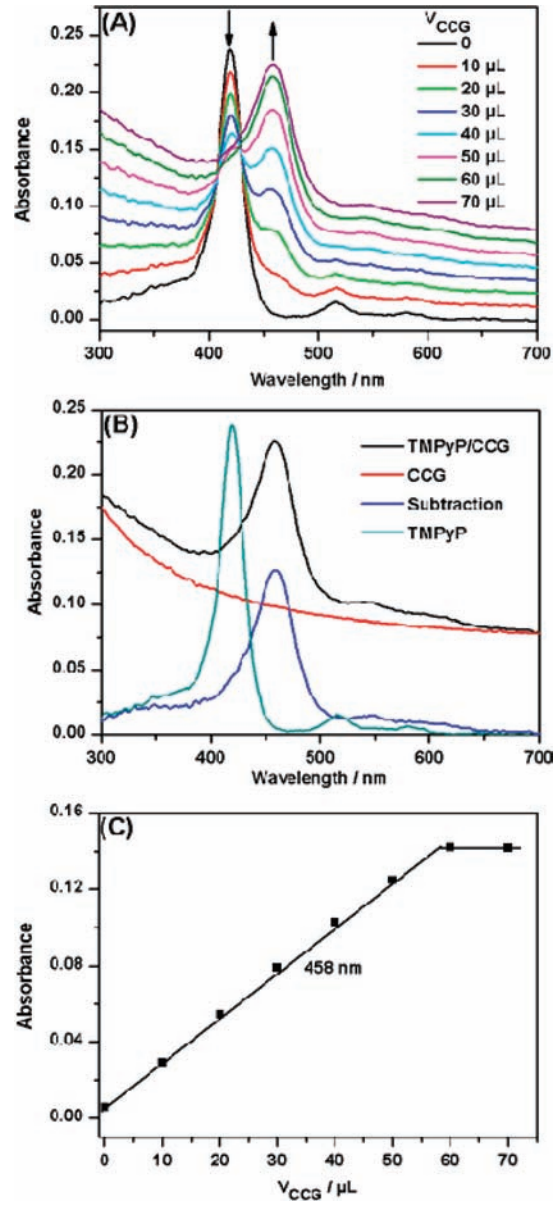


***Figure 1.*** (A) Absorption spectra recorded during the process of titration of 3 mL of 1 $\mu$M aqueous solution of TMPyP with various volumes of 0.25 mg/mL of CCG dispersion ($V_{CCG}$). (B) Absorption spectra of a TMPyP/CCG complex formed at the end point of titration, pure CCG and pure TMPyP solutions, and the subtraction spectrum between the spectra of the TMPyP/CCG complex and CCG (labeled as "Subtraction"). (C) Dependence of absorbance at 458 nm of the subtraction spectrum as a function of volume of CCG dispersion used for titration.

(58) Kano, K.; Minamizono, H.; Kitae, T.; Negi, S. *J. Phys. Chem. A* **1997**, *101*, 6118–6124.
(59) Cady, S. S.; Pinnavaia, T. J. *Inorg. Chem.* **1978**, *17*, 1501–1507.
(60) Chernia, Z.; Gill, D. *Langmuir* **1999**, *15*, 1625–1633.
(61) Kuykendall, V. G.; Thomas, J. K. *Langmuir* **1990**, *6*, 1350–1356.
(62) de Miguel, G.; Perez-Morales, M.; Martin-Romero, M. T.; Munoz, E.; Richardson, T. H.; Camacho, L. *Langmuir* **2007**, *23*, 3794–3801.

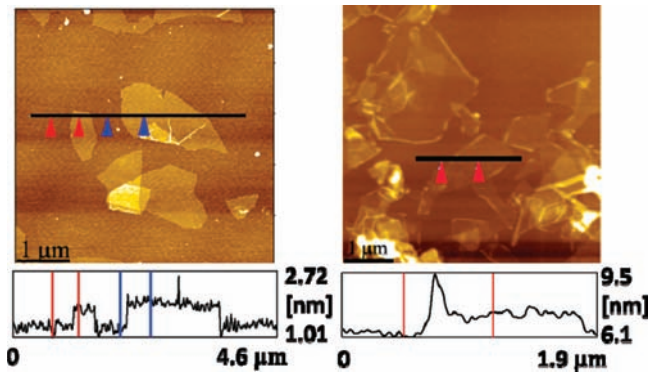


***Figure 2.*** Tapping mode AFM images of exfoliated CCG (left) and TMPyP/CCG complex (right) sheets on mica.

shape and position of the new Soret band at 458 nm, indicating the formation of a new species with well-defined structure. Second, the absorbance at 458 nm read from the subtraction spectrum increases linearly with the amount of CCG dispersion added and finally shows a plateau after addition of 60 $\mu$L or more of CCG dispersion. Third, the absorption spectrum of a TMPyP solid film deposited on quartz glass was recorded for comparison (Figure S3 in the Supporting Information). The Soret band of the solid film showed only a 15-nm red-shift due to J-aggregation of TMPyP molecules. This value is much smaller than that of TMPyP/CCG complex (37 nm) as shown in Figure 1. Last, AFM images of CCG and TMPyP/CCG complex sheets also provided solid evidence for excluding the formation of TMPyP molecular aggregates. As shown in Figure 2, the average thickness of a single-layer CCG sheet was measured to be approximately 0.7 nm, which is consistent with the result reported previously.[12] In comparison, the average thickness of a TMPyP/CCG complex sheet was determined to be about 1.3 nm with 0.6-nm increment compared with that of a clean CCG sheet. Considering the thickness of one TMPyP molecule is about 0.5 nm,[63] we can conclude that the TMPyP molecules were adsorbed on CCG sheets as a monolayer or submonolayer, not aggregates.

On the basis of the results and discussion described above, one can reasonably attribute the large bathochromic shift of the Soret band to the flattening of TMPyP molecules induced by graphene sheets (mechanism (iv)). In the structure of an unstrained TMPyP molecule, four cationic methylpyridinium moieties are nearly perpendicular to the plane of porphyrin because of a strong steric hindrance.[64] When the pyridinium groups rotate toward the coplanar conformation with respect to the porphyrin ring (i.e., flattening), the $\pi$ conjugation and electron-withdrawing effect of TMPyP will be enhanced. As a result, the Soret band of TMPyP shows a large bathochromic shift. Similar phenomenon observed in an anionic clay-cationic porphyrin system also supports this conclusion.[65]

Since TMAP has a molecular structure similar to that of TMPyP, we also titrated the aqueous solution of TMAP with CCG dispersion to further confirm the molecular flattening mechanism. In this case, a similar bathochromic shift of Soret band from 411 to 436 nm and a clear isosbestic point at 416

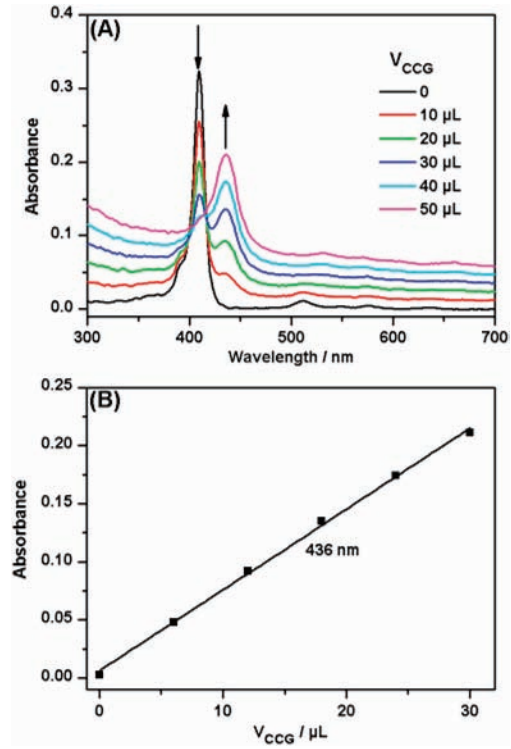


***Figure 3.*** (A) Absorption spectra recorded during the process of titration of 3 mL of 1 $\mu$M aqueous solution of TMAP with 0.25 mg/mL of CCG dispersion. (B) Dependence of the absorbance at 436 nm as a function of the volume of CCG dispersion used for titration.

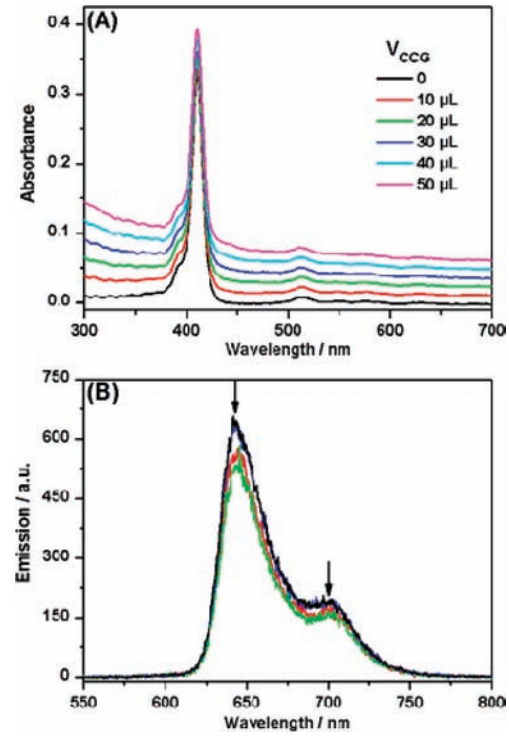


***Figure 4.*** (A) Absorption and (B) fluorescence ($\lambda_{ex}$ = 411 nm) spectra recorded during the process of titration of 3 mL of 1 $\mu$M aqueous solution of TPPS with 0.25 mg/mL of CCG dispersion.

nm were also observed (Figure 3). The absorbance of the new Soret band at 436 nm also increases linearly with the addition of increasing amount of CCG dispersion. The magnitude of bathochromic shift of the Soret band for TMAP (25 nm) is

(63) Wang, H. H.; Han, D. X.; Li, N.; Li, K. E. *J. Inclusion Phenom. Macrocyclic Chem.* **2005**, *52*, 247–252.
(64) Vergeldt, F. J.; Koehorst, R. B. M.; Vanhoek, A.; Schaafsma, T. J. *J. Phys. Chem.* **1995**, *99*, 4397–4405.
(65) Takagi, S.; Shimada, T.; Eguchi, M.; Yui, T.; Yoshida, H.; Tryk, D. A.; Inoue, H. *Langmuir* **2002**, *18*, 2265–2272.

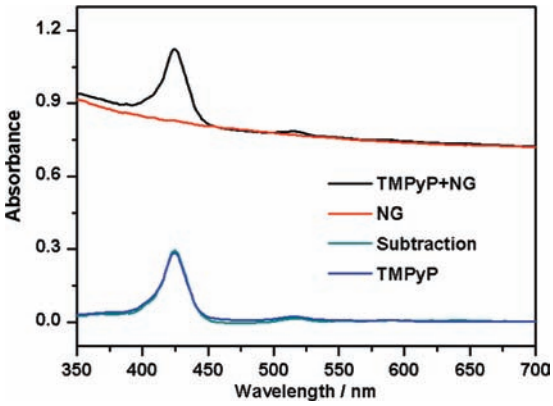


***Figure 5.*** Absorption spectra of the NMP solutions of 0.01 mg/mL of NG, 1 $\mu$M TMPyP, the mixture of 0.01 mg/mL of NG and 1 $\mu$M TMPyP, and the subtraction spectrum derived from the spectra of TMPyP + NG mixture and NG (labeled as "Subtraction").

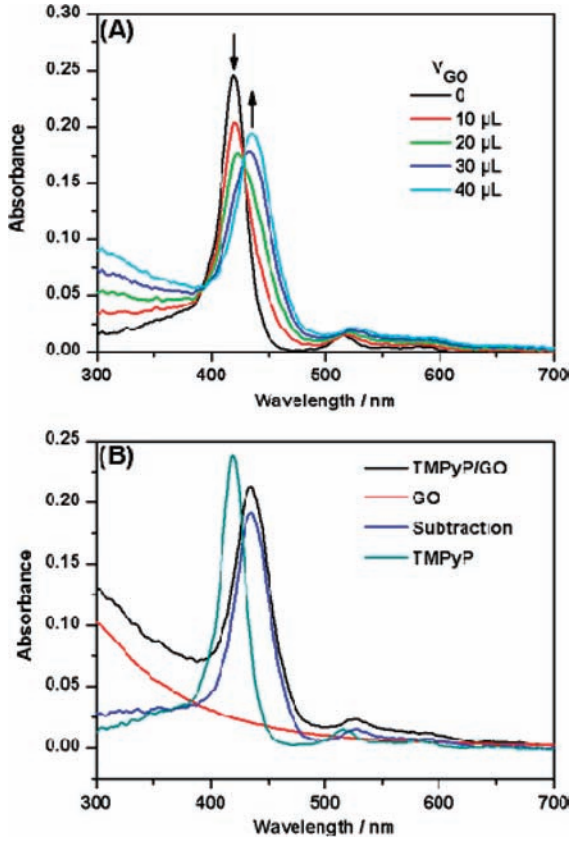


***Figure 6.*** (A) Absorption spectra recorded during the process of titration of 3 mL of 1 $\mu$M aqueous solution of TMPyP with 0.15 mg/mL of GO dispersion. (B) Absorption spectra of TMPyP/GO complex, GO, TMPyP, and subtraction spectrum derived from the spectra of TMPyP/GO complex and GO (labeled as "Subtraction").

smaller than that for TMPyP (37 nm). In the flattening mechanism, the red-shift of the porphyrin Soret band depends on the degree of molecular flattening. Theoretical calculations[60] indicate that ~30 and ~46° twists from vertical direction can cause approximately 30- and 60-nm red-shifts of Soret bands, respectively. The cationic side groups surrounding the porphyrin ring of TMAP are bulkier than those of TMPyP.[65] Therefore, the former porphyrin is more difficult than the latter to be flattened, which will result in a smaller red-shift of Soret band. This result also supports the molecular flattening mechanism.

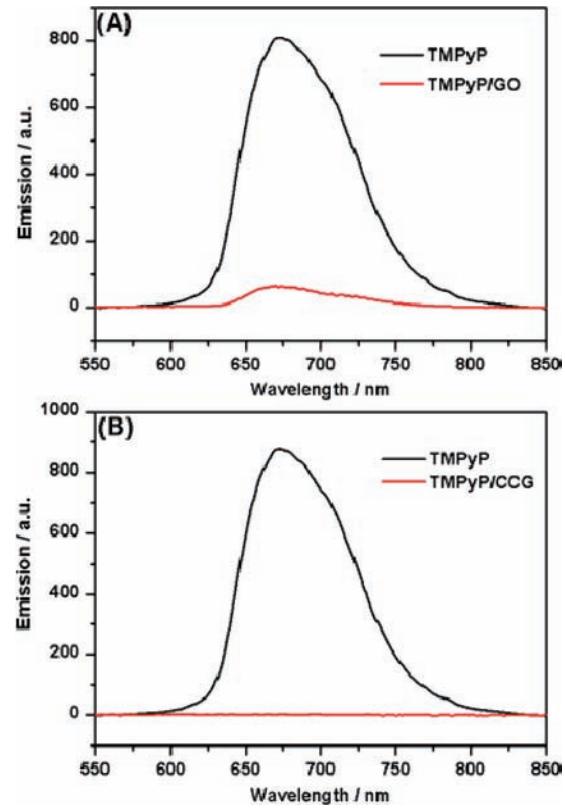


***Figure 7.*** Fluorescence spectra of the aqueous solutions of (A) 1 $\mu$M TMPyP and 1 $\mu$M TMPyP/GO complex (containing 1 $\mu$M TMPyP, $\lambda_{ex}$ = 435 nm) and (B) 1 $\mu$M TMPyP and 1 $\mu$M TMPyP/CCG complex (containing 1 $\mu$M TMPyP, $\lambda_{ex}$ = 458 nm).

***Scheme 1.*** Molecular Flattening of TMPyP Adsorbed on the CCG Sheet

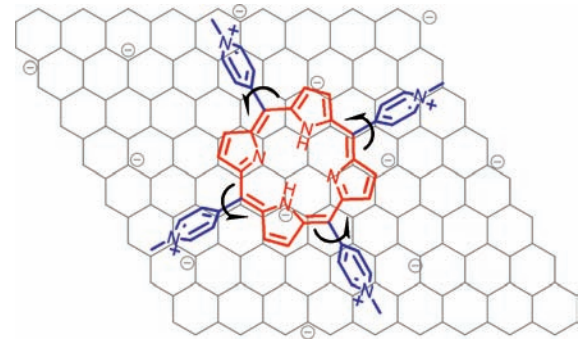

**Driving Forces for Supramolecular Assembly and Flattening of TMPyP Molecules.** As mentioned above, the four cationic methylpyridinium moieties of a TMPyP molecule are nearly perpendicular to the plane of porphyrin because of a strong steric hindrance. Thus, flattening of TMPyP will result in a molecular energy increase in the ground state.[60,64] In view of the compositions and structures of CCG sheets and TMPyP molecules, the driving forces for flattening of TMPyP in TMPyP/CCG complex are expected to be electrostatic and $\pi-\pi$ stacking interactions.

First, the role of electrostatic interaction was studied. When an anionic TPPS aqueous solution was used for replacing a TMPyP solution, the electrostatic attraction in the TMPyP + CCG system was switched to electrostatic repulsion in the TPPS + CCG system. As can be seen from Figure 4A, there are no appreciable spectral changes in UV−visible spectra upon

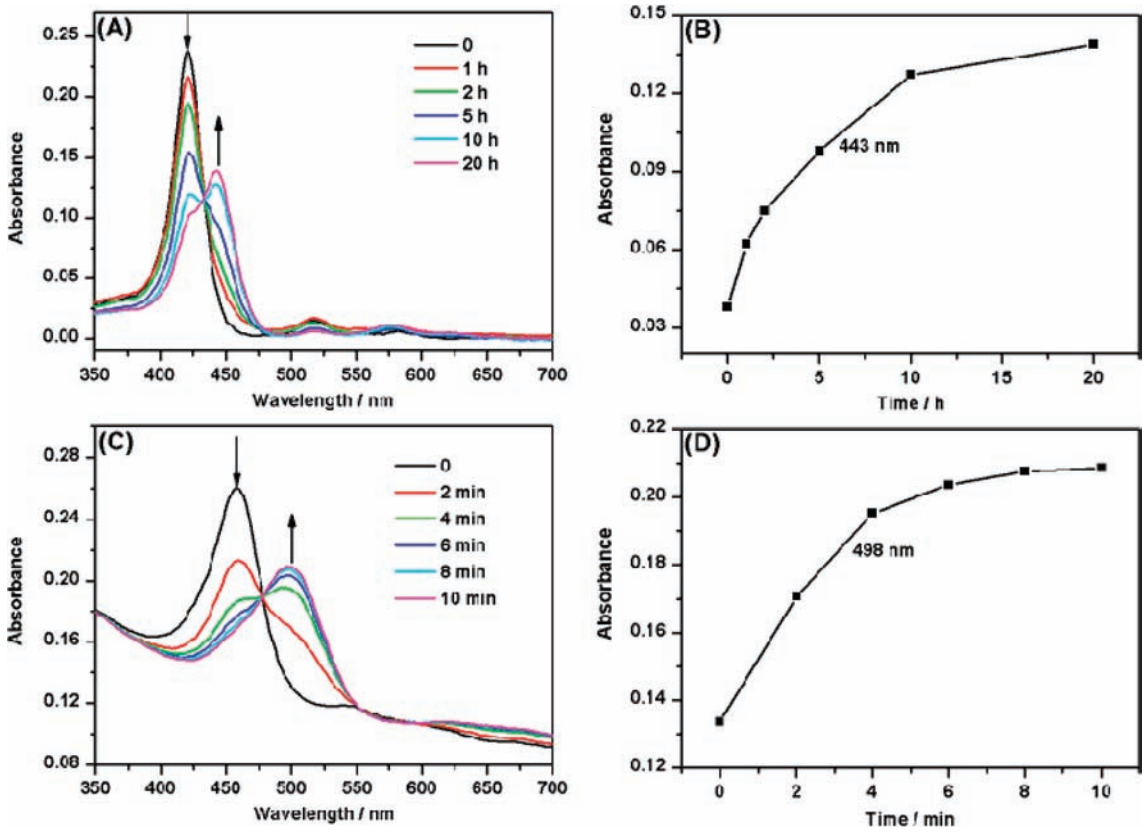


***Figure 8.*** (A) Time-dependent absorption spectra recorded during the reaction of 1 $\mu$M TMPyP and 3 $\mu$M $Cd^{2+}$ ions. (B) Plot of the absorbance at 443 nm versus reaction time based on the spectra shown in (A). (C) Time-dependent absorption spectra recorded during the reaction of 1 $\mu$M TMPyP/CCG complex (containing 1 $\mu$M TMPyP) and 3 $\mu$M $Cd^{2+}$ ions. (D) Plot of the absorbance at 498 nm versus reaction time based on the spectra shown in (C).

titration of TPPS solution with CCG dispersion. Moreover, the fluorescence spectra (Figure 4B) demonstrate that no changes in overall spectral features were detected after variable amounts of CCG dispersion were added, except for a little fluorescence quenching attributed to the competitive light absorption by CCG at the excitation wavelength. Both absorption and fluorescence spectral results reflected that no structural deformation of TPPS was induced by CCG sheets. These results indicate that electrostatic interaction has a strong effect on the supramolecular assembly of TMPyP molecules on CCG sheets.

To further evaluate the effect of electrostatic interaction on the flattening of TMPyP in the TMPyP/CCG complex, the absorption spectra of TMPyP in the absence and the presence of NG sheets with negligible amount of charges were recorded. As seen in Figure 5, the Soret band of TMPyP in NMP is centered at 424 nm, and a 3-nm red-shift relative to that of TMPyP in water is due to solvent effect.[60] After adding 1 $\mu$M TMPyP into 0.01 mg/mL of NG, no visible spectral changes were observed in the subtraction profile, indicating no structural perturbation of TMPyP molecules. It is known that NG sheets bring few charges and still have large conjugated $\pi$ systems.[8] Thus, electrostatic interaction can be ruled out from the system of TMPyP + NG. Comparing the spectral results shown in Figures 1 and 5, it is reasonable to conclude that electrostatic interaction is an indispensable driving force for flattening TMPyP molecules on CCG sheets, at least in the initial stage of assembly.

As the precursor of CCG, GO sheets have smaller conjugated domains and bring more negative charges than those of CCG sheets.[12] Thus, the electrostatic interaction between GO and TMPyP is speculated to be stronger while their $\pi-\pi$ interaction is expected to be weaker than that between CCG and TMPyP. It is reliable to study the effect of $\pi-\pi$ stacking interaction on the flattening of TMPyP by comparing the absorption spectra of TMPyP/GO and TMPyP/CCG complexes. Figure 6 shows the spectral changes of 1 $\mu$M TMPyP upon addition of various volumes of 0.15 mg/mL of GO dispersion. The Soret band of TMPyP in TMPyP/GO complex exhibited only a 14-nm red-shift, and this value is significantly smaller than that observed from the spectrum of the TMPyP/CCG complex (37 nm).

To confirm the differences of $\pi-\pi$ interactions of TMPyP/GO and TMPyP/CCG complexes, fluorescence spectra of the aqueous solutions of TMPyP, TMPyP/GO, and TMPyP/CCG were measured and quantitatively compared (Figure 7). It is clear from the normalized emission spectra shown in Figure 7 that the fluorescence of the porphyrin was greatly quenched in both complexes. The quenching efficiency was calculated to be 93 and 100% for TMPyP/GO and TMPyP/CCG complexes, respectively, indicating that TMPyP molecules have stronger $\pi-\pi$ stacking interactions with CCG sheets than those with GO sheets. The fluorescence quenching may be attributed to the photoinduced electron or energy transfer between TMPyP and GO or CCG.[39,56,66] Therefore, the absorption and fluorescence spectral results signify that the degree of flattening of TMPyP is dependent on the magnitude of $\pi-\pi$ stacking interaction.

On the basis of the spectral results described above, it is reasonable to conclude that the flattening of TMPyP in the TMPyP/CCG complex is triggered by electrostatic and $\pi-\pi$ stacking cooperative interactions. The flattening process shown

(66) Baskaran, D.; Mays, J. W.; Zhang, X. P.; Bratcher, M. S. *J. Am. Chem. Soc.* **2005**, *127*, 6916–6917.

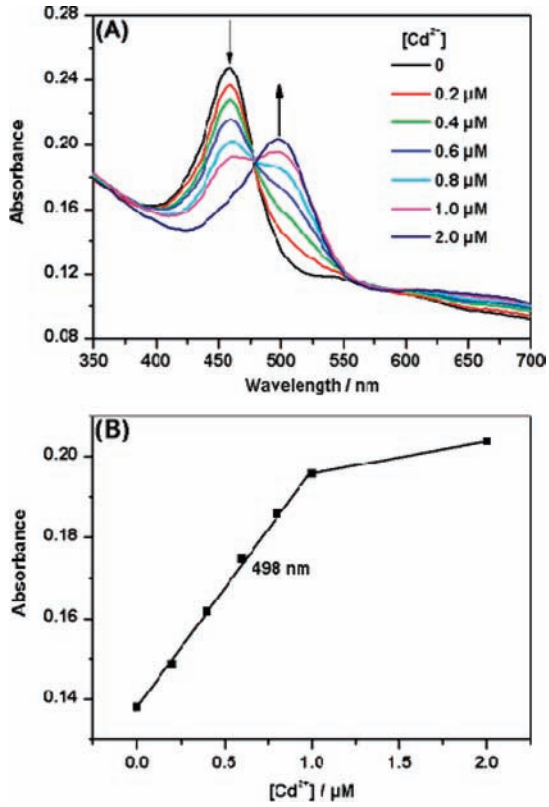


***Figure 9.*** (A) Absorption spectra of 1 $\mu$M aqueous solution of TMPyP/CCG complex (containing 1 $\mu$M TMPyP) in the presence of $Cd^{2+}$ ions with various concentrations (0−2 $\mu$M). (B) Absorbance at 498 nm as a function of $Cd^{2+}$ concentration, $[Cd^{2+}]$.

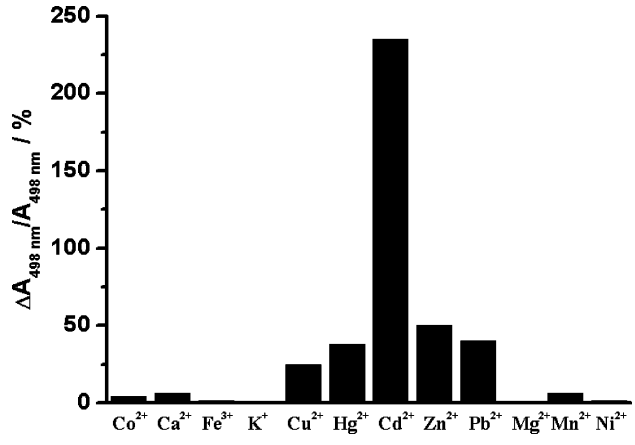


***Figure 10.*** Absorbance changes at 498 nm (subtraction profile) of 1 $\mu$M TMPyP/CCG (containing 1 $\mu$M TMPyP) toward different metal ions with a concentration of 1 $\mu$M each.

in Scheme 1 may be envisaged as follows: TMPyP molecules were first assembled on CCG sheets by electrostatic interaction and then $\pi-\pi$ stacking interaction induced the flattening of TMPyP molecules and enlarged the $\pi$ conjugation of the porphyrin system. The flattening of TMPyP molecules also reduced the distance between the porphyrin planes and CCG sheets, which further enhanced $\pi-\pi$ stacking interaction.

**Accelerated Incorporation of $Cd^{2+}$ Ions into the TMPyP Moieties of TMPyP/CCG Complex.** Various water-soluble porphyrin derivatives including TMPyP have been used for detecting metal ions in aqueous media, because they are simple, inexpensive, and highly sensitive probing molecules for optical analysis.[67] For example, TMPyP has been utilized to detect $Cd^{2+}$ ions.[68] However, the incorporation reaction of the metal ions into the porphyrin ring is slow and the rate of metalloporphyrin formation is several orders of magnitude lower than those with common ligands such as ethylenediamine tetraacetate. This is mainly due to the difficulty in deforming porphyrin ring. Various methods including heating, introducing auxiliary coordination agents, and metal exchange reactions have been proposed to overcome this issue to some extent.[68] As mentioned above, the electrostatic and $\pi-\pi$ stacking cooperative interactions between CCG and TMPyP induced the flattening of TMPyP, which will inevitably deform the porphyrin nucleus because of the large twist of bulky pyridinium substitutes. Therefore, the flattened TMPyP moieties in the TMPyP/CCG complex are expected to accelerate the incorporation of large $Cd^{2+}$ ions into the porphyrin rings. This assumption has been confirmed by the following experiments. As shown in Figure 8A,B, the Soret band of TMPyP at 421 nm is red-shifted to 443 nm after chelating with $Cd^{2+}$ ions. It was found that the coordination reaction of 3 $\mu$M $Cd^{2+}$ and 1 $\mu$M TMPyP solutions under ambient condition needed about 20 h to reach its equilibrium. In a parallel experiment, a new band at 498 nm representing the binding of $Cd^{2+}$ ions into TMPyP/CCG complex was also increased with reaction time and this process under the same conditions took only 8 min to reach its equilibrium, being 150 times faster than that using pure TMPyP solution as a reactant (Figure 8C,D). The bathochromic shift of the Soret band of the TMPyP/CCG complex after binding with $Cd^{2+}$ ions was measured to be 40 nm. This value is nearly twice that (22 nm) determined from the system using pure TMPyP, which further demonstrates the effect of flattening of TMPyP on the coordination reaction of $Cd^{2+}$ ions and the porphyrin molecules. In addition, when a $Cd^{2+}$ ion solution with low concentration (0.2 $\mu$M) was used, this reaction was so fast that the absorbance at 498 nm was stabilized within 2 min after addition of $Cd^{2+}$ ions (Figure S4 in the Supporting Information), indicating the high availability and affinity of TMPyP/CCG complex toward $Cd^{2+}$ ions. To the best of our knowledge, this is the first example of accelerating the coordination reactions between metal ions and porphyrin derivatives by porphyrin molecular flattening.

**Rapid and Selective Detection of $Cd^{2+}$ Ions Using TMPyP/CCG Complex as an Optical Probe.** Figure 9A displays the spectral changes of a 1 $\mu$M aqueous solution of TMPyP/CCG complex in the presence of different concentrations of $Cd^{2+}$ ions. All the spectra were recorded after 10 min of adding metal ions based on the results derived from Figure 8. It is clearly seen from Figure 9B that the absorbance at 498 nm increases linearly with the concentration of $Cd^{2+}$ ions in the range of 0.2−1 $\mu$M (linearly dependent coefficient: $R^2 = 0.997$).

The selectivity of the TMPyP/CCG probe toward $Cd^{2+}$ ions was also studied. We subtracted the normalized CCG contributions from all the absorption spectra of the sensing systems and got the neat absorption spectra of TMPyP moieties of TMPyP/CCG complex and the corresponding metal complexes (Figure S5 in the Supporting Information). Then the ratios of absorbance increment upon addition of metal ions ($\Delta A_{498\ nm}$) to absorbance of pure TMPyP/CCG complex ($A_{498\ nm}$) at 498 nm were plotted against various metal ions, including $Zn^{2+}$, $Hg^{2+}$, $Pb^{2+}$, $Co^{2+}$, $Ni^{2+}$, $Cu^{2+}$, $Mn^{2+}$, $Ca^{2+}$, $Mg^{2+}$, $K^+$, and $Fe^{3+}$. As shown in

(67) Biesaga, M.; Pyrzynska, K.; Trojanowicz, M. *Talanta* **2000**, *51*, 209–224.
(68) Kawamura, K.; Igarashi, S.; Yotsuyanagi, T. *Anal. Sci.* **1988**, *4*, 175–179.

Figure 10, the optical response of the probe toward $Cd^{2+}$ ions is about 4.9, 6.0, and 6.2 times those toward $Zn^{2+}$, $Pb^{2+}$, and $Hg^{2+}$ ions, respectively. The other ions showed negligible disturbances. Although the selectivity of the TMPyP/CCG probe is not as high as some fluorescent probes,[69] it is much better than that using TMPyP as the probe.[68]

## Conclusions

Complexes of TMPyP molecules and CCG sheets have been successfully prepared through supramolecular assembly of both components in aqueous media. The complexation of negatively charged CCG sheets and cationic TMPyP induced a large bathochromic shift (37 nm) of the porphyrin Soret band, mainly due to the molecular flattening of TMPyP. It was verified that the electrostatic and $\pi-\pi$ stacking cooperative interactions between CCG sheets and TMPyP were the main driving forces for complexation and molecular flattening. Furthermore, the flattening of TMPyP in the TMPyP/CCG complex greatly accelerated the coordination reaction of $Cd^{2+}$ ions and TMPyP. TMPyP/CCG complex can be used as a new optical probe for sensing $Cd^{2+}$ ions. The sensor based on this probe exhibited rapid and sensitive responses and improved selectivity toward $Cd^{2+}$ ions. This work provides an example of using colloidal graphene sheets for tuning the structures and functions of porphyrins, and this approach can be extended to other molecules or nanoscale blocks.

**Acknowledgment.** This work was supported by the National Natural Science Foundation of China (50533030, 50873052, and 20774096) and SRFDP (20060003081).

**Supporting Information Available:** Complete ref 8, UV−visible and XPS spectra of CCG and GO, UV−visible spectrum of solid film of TMPyP, UV−visible spectra recorded during the reaction of 1 $\mu$M TMPyP/CCG complex and 0.2 $\mu$M $Cd^{2+}$ ion, and UV−visible spectra of 1 $\mu$M TMPyP/CCG solution in the presence of 1 $\mu$M $Cd^{2+}$ ions or 1 $\mu$M various other metal ions. This material is available free of charge via the Internet at http://pubs.acs.org.

JA905032G

(69) Cheng, T. Y.; Xu, Y. F.; Zhang, S. Y.; Zhu, W. P.; Qian, X. H.; Duan, L. P. *J. Am. Chem. Soc.* **2008**, *130*, 16160–16161.